Int J Adv Manuf Technol (2015) 80:1751–1758
DOI 10.1007/s00170-015-7104-4

ORIGINAL ARTICLE

Determining the minimum clamping force by cutting force simulation in aerospace fuselage pocket machining

A. Mahmud[1] · **J. R. R Mayer**[1] · **L. Baron**[1]

Received: 12 December 2014 / Accepted: 30 March 2015 / Published online: 26 April 2015

Abstract In large fuselage milling operation the panel may deflect and vibrate due to milling thrust force. A clamp is needed on the opposite side of the panel to limit such effects. The support must be able to withstand the thrust force generated by the milling process. In this paper, a specific model for torus cutter milling force and a general milling force model have been simulated to predict the cutting forces. In order to get higher cutting efficiency, the torus cutter needs to adopt different tilt angle relative to the workpiece which changes the thrust force. An equation has been developed to predict the resulting thrust force on the skin panel at different tilting angle. Simulated thrust force results have been validated against dynamometer readings acquired during milling operation.

Keywords Machining · Milling · Clamping force · Torus cutter · Cutter orientation · Cutting force

1 Introduction

This paper describes a model and experiments to determine the minimum clamping force for a mobile magnetic clamp. The magnetic grasping end effector is developed for holding a skin panel during milling operation. The clamping system includes two magnetic modules which are placed either side of the panel.

✉ A. Mahmud
apple.mahmud@ploymtl.ca

J. R. R Mayer
rene.mayer@polymtl.ca

L. Baron
luc.baron@polymtl.ca

[1] Département de génie mécanique, Polytechnique Montréal, C.P. 6079, succ. Centre-ville, Montréal, Canada

Figure 1 shows a general schematic of the grasping machining end effector [3]. Aluminum being a nonmagnetic material the grasping system is constructed by two different magnet module (master and slave) with the orientation of opposite poles (N-S-N-S) on both sides of the panel. The slave magnet module being attracted by the master magnet module will slide over the workpiece (skin panel) and continuously provide sufficient force so that the thin panel does not deflect or deform excessively.

The master module has three cylindrical permanent magnets groups, each group comprising three magnets (Fig. 2). The milling cutter is at the center of the triangle formed by these three magnet sets. The slave module has a similar magnet arrangement. The master and slave work together as a clamp. An ultrasonic thickness sensor continually measures the thickness of the skin panel and corresponding depth of cut is adjusted in the one axis spindle to maintain a constant remaining floor thickness.

A magnetic clamp which must withstand the thrust force from the milling operation also needs to move smoothly with low frictional force. Excessive clamping force creates large friction forces which hinder the sliding of the clamp. Clamping force needs to be optimized so that the clamp can provide sufficient support force against the milling thrust force while allowing the clamp to move against the frictional force. Higher clamping force helps to stabilize the fixture in out-of-plane motion but reduces the in-plane mobility motion due to increased frictional forces and may damage the panel surface.

Several camping force optimization technique have been proposed. The finite-element (FE) modeling approach is very common in fixture design and clamping force optimization for machining operation. Most of the work has the drawback of large model size requiring higher computation cost. A more computationally efficient method [8] where one genetic algorithm-based fixture layout and clamping force optimization method has been speeded up by a matrix size-reducing method for solving FEM balance equation.

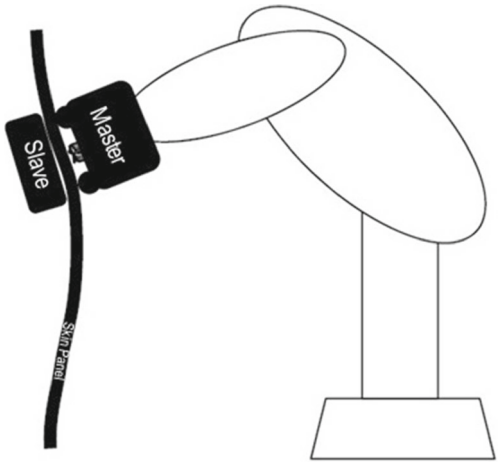

Fig. 1 General schematic diagram of the grasping machining end effector concept

Rigid-body modeling which considers both the workpiece and the fixture as perfectly rigid solids has been applied [12] to solve the problem of clamping force optimization. An elastic method has been used to model workpiece-fixture deformation. Li and Melkote [7] estimated optimum clamping forces for a multiple clamp fixture subjected to quasi-static machining forces by solving a multi-objective constrained optimization model. The algorithm for clamping force optimization represents the fixture-workpiece contact as elastic contacts.

An unconstrained nonlinear programming technique has been used to predict contact forces by Xiong et al. [13] and constrained quadratic optimization programming has been used by Wang and Pelinescu [12] to estimate the contact forces for known clamping force. Trappey and Liu [11] solved quadratic model of clamping forces including contact force by nonlinear programming whereas Qin et al. [9] feasibly slacked constrained quadratic optimization into constrained linear programming problem to determine required clamping force to stabilize the workpiece.

Particle swarm optimization (PSO) techniques featuring computational intelligence has been used for clamping force optimization by Deng and Melkote [4]. The clamping force optimization problem was formulated as a bi-level constrained nonlinear programming problem to find the "best" set of clamping forces swiftly.

Balancing force-moment method and the Coulomb's static friction law were used to determine minimum clamping force to hold the workpiece without deformation by Selvakumar et al. [10]. The optimum clamping force is selected as the maximum clamping forces calculated from five different tool positions with respect to the workpiece.

All the above-mentioned clamping force optimization method assume the workpiece and clamping fixture are in static contact with no relative displacement. In case of a mobile magnetic clamp which slides over the workpiece (fuselage skin panel) also must provide sufficient clamping force to withstand milling thrust force. So these solutions are not applicable for a mobile magnetic clamping fixture.

In milling operation cutter axis tilting is common which changes the axial thrust force by adding the projection of tangential and radial forces to the axial thrust force. The paper analyses the thrust force generated by the milling cutter at different tilt angles and takes the maximum thrust force as the minimum clamping force. For this purpose, a torus milling cutter forces is simulated varying the inclination angle and the prediction verified experimentally.

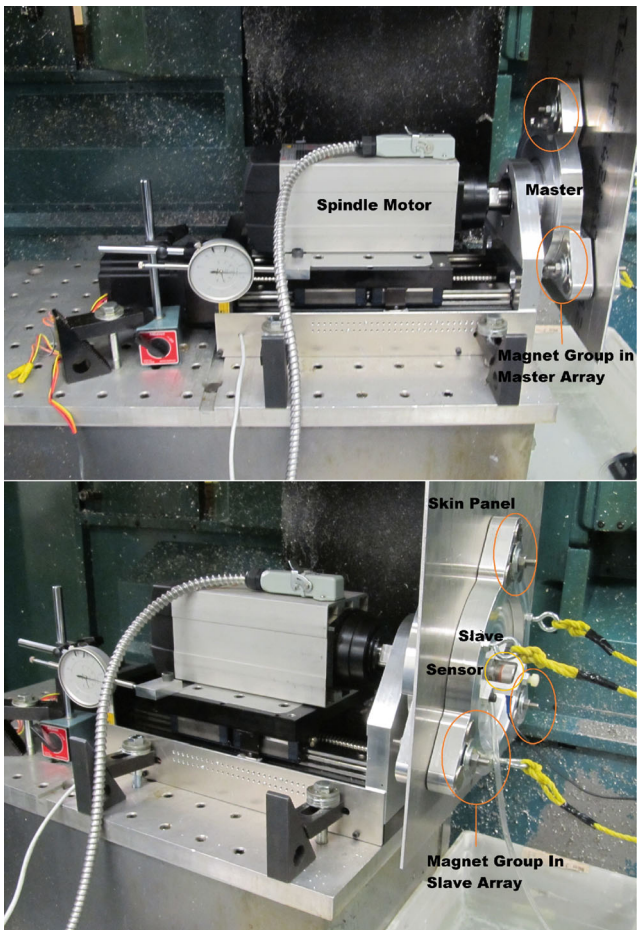

Fig. 2 Master and slave magnet module clamp the non-magnetic aluminum skin panel

2 Thrust force model

Using a toroidal tool and appropriate tilting and cutting tool displacement direction in relation to surface curvature improves the cutting efficiency [2]. Since this tilted tool axis introduces different thrust force to the milling surface compared to the perpendicular situation, it is important to understand and quantify the forces in order to design the clamping device.

Altintas and Lee [1] expressed cutting forces as a function of cutting pressure exerted on the instantaneous uncut chip area.

$$\begin{aligned} F_t(\theta) &= K_t(\theta) * d_a * f_t \sin(\theta) \\ F_r(\theta) &= K_r * F_t(\theta) \\ F_a(\theta) &= K_a * F_t(\theta) \end{aligned} \tag{1}$$

Where f_t is the feed per tooth, d_a is the axial engagement, and θ is the angular (around the tool axis) position of the torus cutter. The cutting force coefficient $K_t(\theta)$ depends on the material characteristics and cutter geometry. K_r and K_a coefficients are calculated from the ratios of maximum radial to tangential and axial to tangential forces, respectively.

Gilles et al. [5] expressed this cutting coefficient for torus milling cutter as a combination of two different coefficients K_{to} and β.

$$K_t(\theta) = K_{to}(\text{emoy}(\theta))^{\beta} \tag{2}$$

where the average chip thickness emoy(θ) is the function of the cutting parameter and the cutter geometry (Fig. 3).

$$\begin{aligned} \text{emoy}(\theta) &= \frac{f_t \sin(\theta) * d_a}{r\left(\pi/2 - \phi\right)} \\ \text{with} \quad \phi &= \sin^{-1}\left(\frac{r - d_a}{r}\right). \end{aligned} \tag{3}$$

The average chip thickness emoy depends on the axial engagement d_a. If the cutter axis has a negative tool axis inclination [6], axial engagement also changes. To maintain the constant depth of cut, p, the axial engagement changes (Fig. 4).

$$\begin{aligned} d_a &= \left(p - \frac{\delta}{2}\right) + \frac{\delta}{2}\sin(\theta),\ d_a(\leq 0) = 0 \\ \delta &= (D - 2r)\sin(\alpha) \end{aligned} \tag{4}$$

where D is the tool diameter, r is the round insert radius, and α is the inclination angle. Any negative d_a value indicates no axial engagement.

A logarithmic residue matrix method has been established to calculate coefficient K_{to} and β of Eq. (2) by Gilles et al. [5]

$$\begin{aligned} &\begin{pmatrix} \text{Number of points} & \sum_i \log(\text{emoy}(\theta_i)) \\ \sum_i \log(\text{emoy}(\theta_i)) & \sum_i \log(\log(\text{emoy}(\theta_i)))^2 \end{pmatrix}_{2x2} \\ &\times \begin{pmatrix} \log(K_{to}) \\ \beta \end{pmatrix} \\ &= \begin{pmatrix} \sum_i^{2x1} \log(F_{t_i}) \\ \sum_i [\log(F_{t_i}) \log(\text{emoy}(\theta_i))] \end{pmatrix}_{2x1} \\ &- \begin{pmatrix} \sum_i \log(d_a f_t \sin(\theta_i)) \\ \sum_i [\log(d_a f_t \sin(\theta_i)) \log(\text{emoy}(\theta_i))] \end{pmatrix}_{2x1} \end{aligned} \tag{5}$$

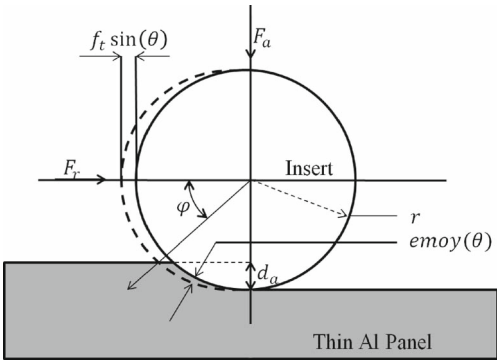

Fig. 3 Average chip thickness emoy(θ) and axial engagement d_a

Assuming α is around an axis perpendicular to the feed direction and let us say this is the X-axis, then $R_x(\alpha)$ is the rotation matrix describing the tilt action on the tool body.

$$R_x(\alpha) = \begin{vmatrix} 1 & 0 & 0 \\ 0 & \cos(\alpha) & -\sin(\alpha) \\ 0 & \sin(\alpha) & \cos(\alpha) \end{vmatrix} \tag{6}$$

Then defining the tool axis as the Z-axis resulting from α the rotation matrix about the Z-axis is $R_z(\theta)$.

$$R_z(\theta) = \begin{vmatrix} \cos(\theta) & -\sin(\theta) & 0 \\ \sin(\theta) & \cos(\theta) & 0 \\ 0 & 0 & 1 \end{vmatrix} \tag{7}$$

Calculated cutting forces $F_t(\theta)$ $F_r(\theta)$, and $F_a(\theta)$ in the local (tool) reference frame are projected in the workpiece fixed reference. Considering the tool rotation about the Z-axis and tilting angle about X-axis cutting force components in workpiece frame are $F_x(\alpha)$ $F_y(\alpha)$, and $F_z(\alpha)$.

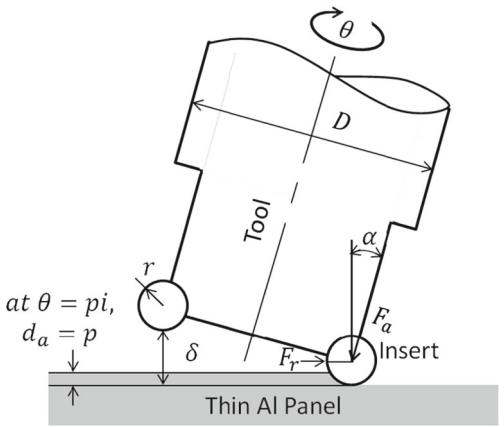

Fig. 4 Axial engagement d_a for constant depth of cut p

$$\begin{bmatrix} F_x(\alpha) \\ F_y(\alpha) \\ F_z(\alpha) \end{bmatrix} = \begin{vmatrix} 1 & 0 & 0 \\ 0 & \cos(\alpha) & -\sin(\alpha) \\ 0 & \sin(\alpha) & \cos(\alpha) \end{vmatrix} \times \begin{vmatrix} \cos(\theta) & -\sin(\theta) & 0 \\ \sin(\theta) & \cos(\theta) & 0 \\ 0 & 0 & 1 \end{vmatrix} \times \begin{bmatrix} F_r(\theta) \\ F_t(\theta) \\ F_a(\theta) \end{bmatrix} \tag{8}$$

$$= \begin{vmatrix} \cos(\theta) & -\sin(\theta) & 0 \\ \cos(\alpha)\sin(\theta) & \cos(\alpha)\cos(\theta) & 0 \\ \sin(\alpha)\sin(\theta) & \sin(\alpha)\cos(\theta) & \cos(\alpha) \end{vmatrix} \times \begin{bmatrix} F_r(\theta) \\ F_t(\theta) \\ F_a(\theta) \end{bmatrix} \tag{9}$$

Clamping forces in all three directions are important. However the magnetic chuck [3] aims at counteracting the Z-axis force to support the thin panel from the rear side. So the Z-axis force only is considered from now on.

The thrust force $F_z(\alpha)$ is the force that the milling cutter applies to the milled object in the out-of-plane direction. The thrust force depends on the tool inclination angle. Tilting caused change in inclination angle. Tilting angle α theoretically could vary from 0 to 90°.

$$F_z(\alpha) = \sin(\alpha)\sin(\theta) * F_r(\theta) + \sin(\alpha)\cos(\theta) * F_t(\theta) + \cos(\alpha) * F_a(\theta) \tag{10}$$

$F_z(\alpha)$ can be expressed including K_r and K_a coefficients using 1.

$$F_z(a) = F_t(\theta)(\sin(a)\sin(\theta) * K_r + \sin(\alpha)\cos(\theta) + \cos(\alpha) * K_a) \tag{11}$$

3 Experimental setup

A Kistler dynamometer has been installed on a 5-axis CNC machine (HURON KX8 – 5 axes). A torus cutter (model-ER D038A075-2-MIO-0.38) is fixed to the spindle which rotates at 5000 rpm. On the tool (diameter, D=19.05 mm) one of the two inserts (radius, r=9.652 mm) is removed to perform a single insert milling operation.

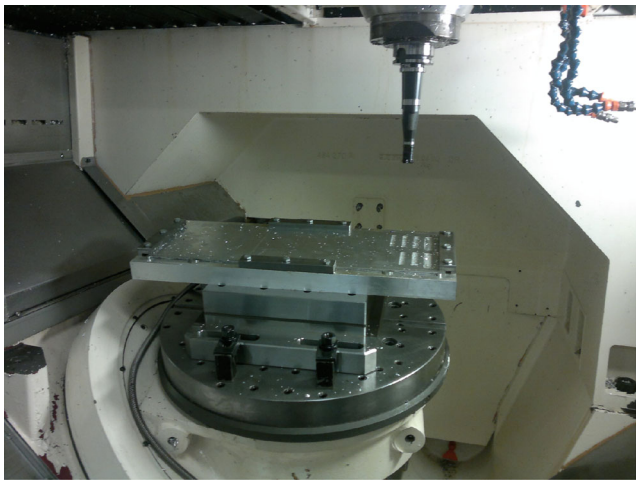

Fig. 5 Kistler dynamometer fixed on the CNC machine bed (model-HURON KX8)

Milling is performed with a feed rate of 400 mm/min in air cooling. The single insert resulted in a feed per tooth f_t= 0.08 mm. A thin aluminum (AL2024-T3) plate is placed on top of the dynamometer using a specially designed fixture.

The dynamometer is connected to a data acquisition system, PXI 1006B chassis including two 8-channel cards PXI 4472 via the amplifier. The computer shows the measured force in a Lab View VI shown in Figs. 5 and 6.

The dynamometer measures three forces in the fixed workpiece reference frame (X, Y, and Z) in three 2D graphs. Data are also recorded as a .txt file for further analysis. The sampling frequency of the force data acquisition was 1000 Hz (Fig. 7).

Fig. 6 LabView based data acquisition system with Kistler dynamometer

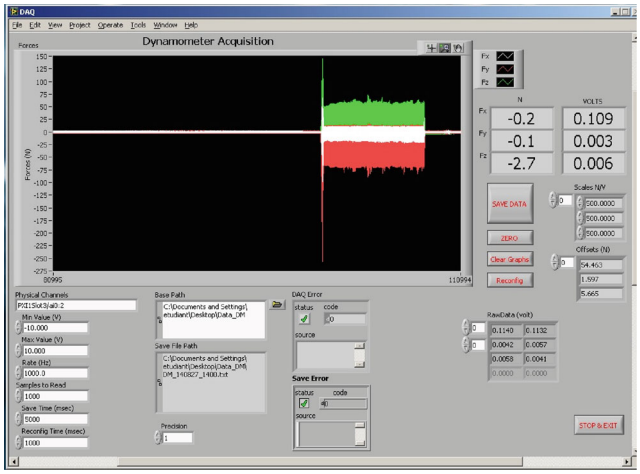

Fig. 7 Measured forces F_x, F_y, and F_z in fixed workpiece reference frame

4 Simulated thrust force

The cutting force data measured by the Kistler dynamo meter is in the fixed wokpiece framework with three cutting force components F_x, F_y, and F_z. Tangential, radial, and axial forces on the local (tool) frame are $F_t(\theta)$, $F_r(\theta)$ and $F_a(\theta)$.

At 0° inclination (α=0), Eq. (9) takes the form

$$\begin{bmatrix} F_x(\alpha) \\ F_y(\alpha) \\ F_z(\alpha) \end{bmatrix} = \begin{bmatrix} \cos(\theta) & -\sin(\theta) & 0 \\ \sin(\theta) & \cos(\theta) & 0 \\ 0 & 0 & 1 \end{bmatrix} \times \begin{bmatrix} F_r(\theta) \\ F_t(\theta) \\ F_a(\theta) \end{bmatrix} \quad (12)$$

The experimental setup measures forces in fixed reference system which needs to be converted to forces in local frame. Inverse matrix helps to switch from fixed reference frame to local frame (Fig. 8).

$$\begin{bmatrix} F_r(\theta) \\ F_t(\theta) \\ F_a(\theta) \end{bmatrix} = \begin{bmatrix} \cos(\theta) & \sin(\theta) & 0 \\ -\sin(\theta) & \cos(\theta) & 0 \\ 0 & 0 & 1 \end{bmatrix} \times \begin{bmatrix} F_x(\alpha) \\ F_y(\alpha) \\ F_z(\alpha) \end{bmatrix} \quad (13)$$

The experimentally measured forces $F_x(\theta)$, $F_y(\theta)$, and $F_z(\theta)$ are plotted using Matlab and then rotation matrix calculates the radial $F_t(\theta)$ tangential $F_r(\theta)$ and axial $F_a(\theta)$ forces on the local (tool) reference system (Fig. 9).

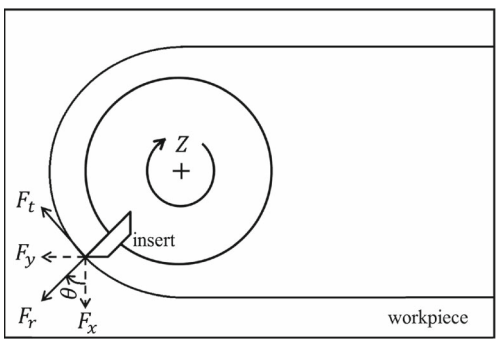

Fig. 8 Fixed workpiece reference system to local reference system force components conversion

Forces in local (tool) reference system could be effectively used to calculate the two model parameters K_{to} and β by (4). Calculated values for K_{to}=785.94 MPA and β=−0.2210

Average chip thickness emoy(θ) is calculated from axial engagement d_a based on the tool axis inclination angle α and tool rotation angle, θ. Without any tilting (inclination angle, α=0) axial engagement d_a remains equal to the required depth of cut p. As soon as tilting increases, axial engagement changes with tool rotation.

Figure 10 shows that for a constant depth of cut of 0.5-mm axial engagement changes from 0 to 0.5 mm at different rotation angle. Based on Eq. (3), the corresponding emoy (average chip thickness) has been calculated.

Finally Eq. (2) is used to calculate $K_t(\theta)$. Ratios of maximum radial to tangential and axial to tangential forces, respectively, determine K_r and K_a. These two ratios have been identified by Eq. (1)

$$K_r = 0.4090 \; K_a = 0.7308$$

With all the available data of cutting force coefficient, axial engagement, radial to tangential and axial to tangential ratios Eq. (1) can simulate all three radial tangential and axial forces without considering any tool inclination. These simulated cutting forces have been transformed to fixed reference frame for comparing to the force data acquired at 0° tilting milling operation, α=0.

At 0° inclination, the measured average maximum axial forces for a 0.5-mm depth of cut is 55.60 N whereas the calculated axial force based on Gilles's formula is 55.73 N (Fig. 11).

The main interest of this work is to estimate the thrust force on the milling surface. Without any inclination, the thrust force is straightforward and is calculated as the axial. As soon as the cutter axis is tilted, i.e., α is increased, both the

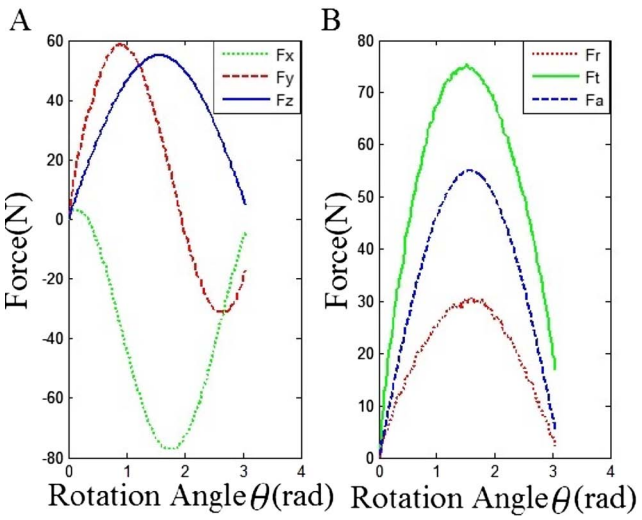

Fig. 9 Experimental force data (**a** fixed workpiece reference) calculated force data (**b** local reference system) at a=0 °

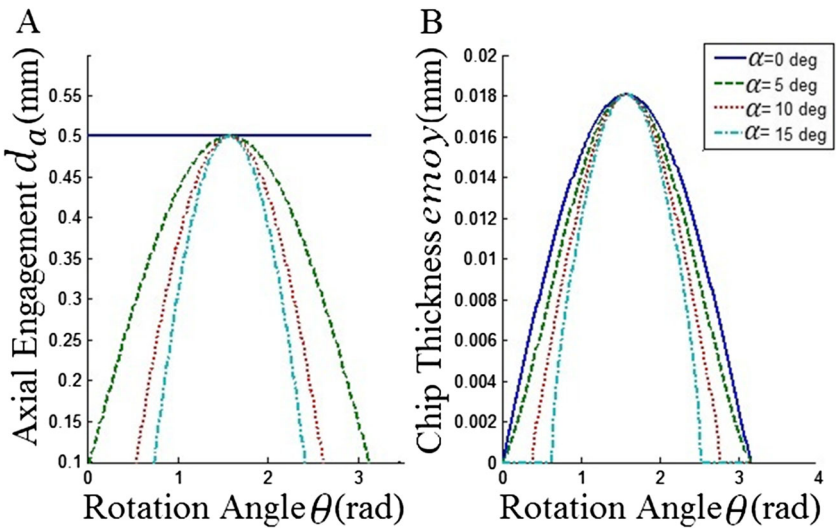

Fig. 10 **a** Axial engagement, d_a. **b** Average chip thickness, emoy at different tilting angle (a = 0, 5, 10, 15 °)

tangential and radial forces influence the axial force by a factor of sin(α). At the same time, axial force itself gets reduced by a factor of cos(α) as seen in Eq. (10).

To verify the combined effect, these sin(α) and cos(α) factors on the thrust force three different tests were accomplished at tilting angles 5, 10, and 15°.

Equation (11) predicts the thrust force. The average maximum thrust force was 55.60 N without any tilting angle; only a 5° tilting changes the amount to 57.77 N, which is close to the simulated maximum axial force of 58.53 N (Fig. 12). A further tilting of 5° (α=10 °) increases the thrust force to 60.10 N. Simulated thrust force at 10° tilting is 60.98 N (Fig. 13).

In a five axis CNC milling operation 10 to 15° tilting angle is very common. An additional test being performed at 15° inclination shows a further increased thrust force to 62.60 N, matched by the simulated maximum force of 62.95 N (Fig. 14).

After measuring 0 (without any tilting) to 15° tilting angle and their corresponding thrust forces, it is necessary to get the trend how tilting angle influences the thrust force and what is the maximum possible thrust force. All theoretically possible tilting angles have been simulated at 1° interval and the corresponding maximum thrust forces plotted in (Figs. 15).

Simulations yield a maximum thrust force of 65.99 N at an inclination angle of 34° (α=34 °). Theoretically, this force needs to be supported by a clamping fixture so that the workpiece remains in position while milling.

5 Results and verification

Theoretically, the tilting angle could be wide range from 0 to 90°. But in reality, the tilting angle does not need to be so extreme. A moderate tilting angle could be 10 to 15°. And specially the magnetic milling device for which this chuck is been designed can only attain a 10 to15° tilting at its best. So experiments were also conducted up to 15° inclination.

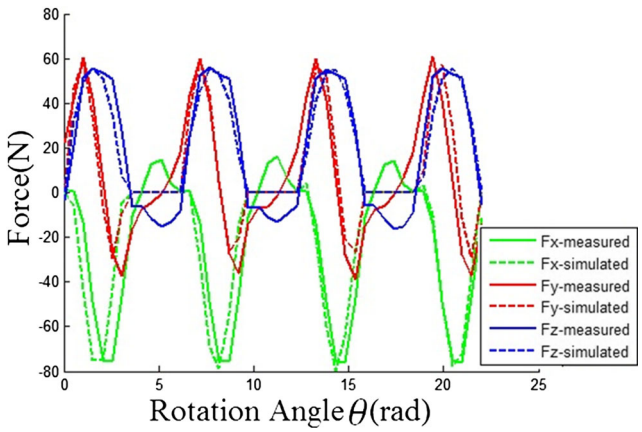

Fig. 11 Simulated verses measured cutting forces with no tilting angle (a=0 °) in fixed framework

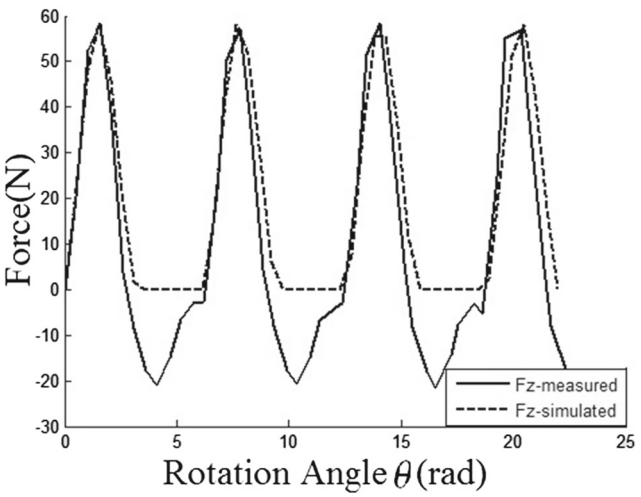

Fig. 12 Thrust force at 5° tilting angle (a=5 °)

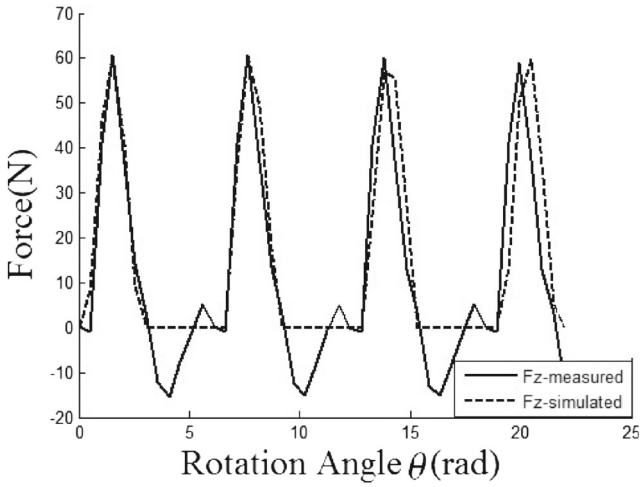

Fig. 13 Thrust force at 10° tilting angle (a=10 °)

The same method could be applied for predicting maximum thrust force multiple teeth milling cutter by changing corresponding material characteristics and geometric data.

6 Conclusion

Whereas clamping on the panel periphery is imparted to support gravitational and inertial forces, the cutting force requires local support of the panel. A magnetic clamp for local support needs to provide sufficient force to keep the panel in position. If the magnetic clamp can support the maximum milling thrust force, the fuselage skin panel will be correctly held.

Since torus cutter offers the probability of higher material removal rate by the tilting of the tool with respect to the panel surface, in this paper, a methodology has been established to predict the maximum thrust force produced from this cutting operation. First of all, considering the cutter geometry and cutting operation variable (depth of cut, rpm, tool inclination, or tilt), thrust forces have been simulated. Evaluating all the

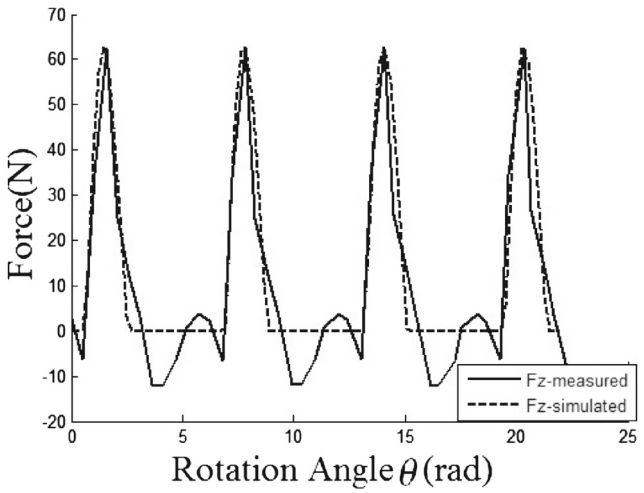

Fig. 14 Thrust force at 15° titling angle (a=15 °)

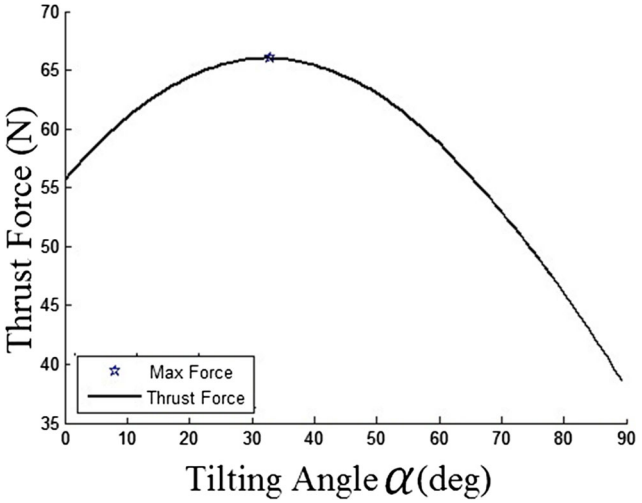

Fig. 15 0 to 90° tilt angle and corresponding thrust force

possible thrust force at different tilting angle, the maximum force is determined. The maximum thrust force for this specific milling case was 66 N is the minimum clamping force for the magnetic clamp design.

In future work, friction force between the skin panel and the clamping unit of both the master and slave sliding over the skin panel needs to be considered. Alternative selection between minimum radius contact ball avoiding Hertzian effect or low friction pad would be necessary to ensure a smooth motion against friction.

Acknowledgments This work was supported by the project "Machining of skin panels (Al or Al-Li)," CRIAQ MANU-412–NSERC RDCPJ 411911-10).

References

1. Altintas Y, Lee P (1998) Mechanics and dynamics of ball end milling. J Manuf Sci Eng 120(4):684–692
2. Balazinski MS, Gravelle, et al (1998) Evaluation of the distance between the machining of assists for the tool tip-ring. 2nd International Conference on Designing and Manufacturing Integrated Mechanical IDMME'98 Compiegne, France: May 27-29 pp 569-575
3. Chouinard A (2011) Remplacement de l'usinage chimique des tooles aeronautiques minces en aluminium par de l'usinage mecanique. Departement de genie mecanique, Ecole Polytechnique de Montreal. M Sc
4. Deng H, Melkote SN (2006) Determination of minimum clamping forces for dynamically table fixturing. Int J Mach Tool Manuf 46(7):847–857
5. Gilles P, Monies F et al (2006) Modelling cutting forces in milling on torus cutters. Int J Mach Mach Mater 1(2):166–185
6. Gilles P, Monies F et al (2007) Optimum orientation of a torus milling cutter: method to balance the transversal cutting force. Int J Mach Tool Manuf 47(15):2263–2272
7. Li B, Melkote S (2001) Fixture clamping force optimisation and its impact on workpiece location accuracy. Int J Adv Manuf Technol 17(2):104–113

8. Liu Z, Wang MY, et al (2012) One fast fixture layout and clamping force optimization method based on finite element method. ASME/ISCIE 2012 International Symposium on Flexible Automation, American Society of Mechanical Engineers
9. Qin G, Lu D, et al (2009) A slack-based method to clamping force optimization for fixture design. Information and Automation, 2009. ICIA'09. International Conference on, IEEE
10. Selvakumar S, Arulshri KP, Padmanaban KP, Sasikumar KSK (2010) Clamping force optimization for minimum deformation of workpiece by dynamic analysis of workpiece-fixture system. World Appl Sci J 11(7):840–846
11. Trappey A, Liu C (1992) An automatic workholding verification system
12. Wang MY, Pelinescu DM (2003) Contact force prediction and force closure analysis of a fixtured rigid workpiece with friction. J Manuf Sci Eng 125(2):325–332
13. Xiongand C-H, Xiong Y-L, et al (2003) On prediction of passive contact forces of workpiece-fixture systems. ASME 2003 International Design Engineering Technical Conferences and Computers and Information in Engineering Conference, American Society of Mechanical Engineers